STATE OF VAPOR – GAS BUBBLES IN THE ARTERIES OF LOW-TEMPERATURE HEAT PIPES

M. N. Ivanovskii, V. V. Privezentsev, and V. P. Sorokin

UDC 621.036.2

Investigations into the behavior of vapor–gas bubbles in artery channels have been conducted to analyze the capabilities of low-temperature increased-power heat pipes. A method for removing the bubbles from the artery system is suggested and experimentally confirmed.

The working liquids of low-temperature heat pipes have very fair thermophysical properties. The hydrodynamic pressure losses in the liquid usually dominate in the total pressure drop along the liquid–vapor–liquid circuit. Therefore, it is an important task in increasing the heat transfer for such pipes to develop a high-efficiency capillary structure which, on the one hand, would have a large capillary head, and on the other hand, low resistance to condensate flow. The perfect solution to this problem would be arterial capillary systems in which these two factors are not interdependent.

Low-temperature arterial heat pipes have already found use in the space research field [1-3], where the absence of gravity facilitates the process of filling the arteries with liquid. However, wide use of these capillary systems is limited by a number of difficulties, which have not as yet been finally resolved. The main problem is the matter of continuously filling the arteries with liquid heat-transfer agent, and the associated problem of removing (or dissolving) vapor–gas bubbles [4, 5], as well as the matter of stable operation of heat pipes with this type of capillary system [6].

1. Theoretical Analysis of the Equations of State for Vapor–Gas Bubbles. Vapor–gas bubbles can form when the wick is being filled with condensate, and also during startup and operation of heat pipes. The mechanism for formation of bubbles, arising during the filling of the wick with heat transfer agent, has been described in [7]. In gas-filled pipes, bubbles can also be formed during operation of the pipe because of desorption, boiling or oscillations of the vapor-gas front in the condenser [6, 8, 9]; i.e., even though the artery filling process has not generated bubbles, the introduction of noncondensible gas into the tube may cause a drop in its heat transfer. Experimental proof of this phenomenon was presented in [8].

We require to find the main criteria governing the behavior of vapor–gas bubbles. In the analysis it is desirable to use the same principles which were used by the author of [10] in determining the criteria for boiling on a surface. The size of the bubble, the concentration of gas in the bubble, the temperature superheat, and also the gravitational and circulatory pressure drops in the heat pipe determine the growth, equilibrium or collapse of a bubble. The mechanical equilibrium equation at the vapor–liquid interface in the bubble has the form

$$P_{\text{vB}} + P_{\text{gas}} = P_l + \Delta P_\sigma. \tag{1}$$

The partial vapor pressure in the bubble is given by the relation

$$P_{\text{vB}} = P_l + \Delta P_i, \tag{2}$$

where ΔP_i is the excess vapor pressure due to the temperature superheat ΔT_B of the liquid surrounding the bubble, and also to the gravitational and circulatory pressure drop

$$\Delta P_i = \Delta P_g + \Delta P_l + \Delta P_T. \tag{3}$$

The sum of the gravitational and circulatory pressure drops can be expressed in terms of the effective radius R_{ef} of curvature of the meniscus at the interphase boundary in the artery-vapor channel:

$$\Delta P_g + \Delta P_l = \frac{\sigma}{R_{\text{ef}}}. \tag{4}$$

Translated from Inzhenerno-Fizicheskii Zhurnal, Vol. 35, No. 4, pp. 591-599, October, 1978. Original article submitted October 5, 1977.

0022-0841/78/3504-1144$07.50

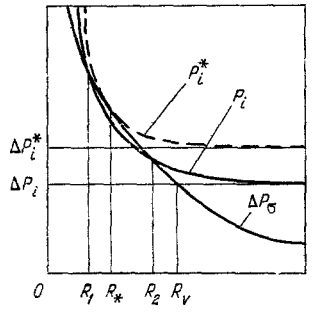

Fig. 1

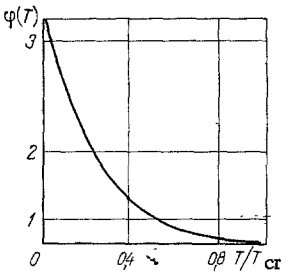

Fig. 2

Fig. 1. The forces acting on a vapor–gas bubble as a function of the radius R.

Fig. 2. The temperature dependence of the function $\varphi(T)$ for the heat-transfer agents Freon 14 and Freon 22. The quantity T/T_{cr} is the relative temperature.

The pressure drop due to overheat can be approximated by the expression

$$\Delta P_T = \left(\frac{\partial P}{\partial T}\right)_s \Delta T_в; \tag{5}$$

Thus, the excess vapor pressure can be represented in the form

$$\Delta P_i = \frac{\sigma}{R_{ef}} + \left(\frac{\partial P}{\partial T}\right)_s \Delta T_в. \tag{6}$$

By introducing the excess pressure of the vapor–gas mixture

$$P_i = \Delta P_i + P_{gas}, \tag{7}$$

Eq. (1) for the mechanical equilibrium can be written in the form

$$\Delta P_i = \Delta P_\sigma. \tag{8}$$

The state of a spherical vapor–gas bubble is given by the Clapeyron–Mendeleev equation

$$P_{gas} = b/R^3, \tag{9}$$

where

$$b = \frac{3\bar{R}}{4\pi} mT. \tag{10}$$

Taking into account the last relations, Eq. (8) takes the form

$$\Delta P_i + \frac{b}{R^3} = \frac{2\sigma}{R}. \tag{11}$$

If the excess vapor pressure $\Delta P_i \leq 0$, the last equation has the unique solution $R = R_1$, which describes a stable state of the bubble. A bubble formed during charging has a stable form. If $\Delta P_i > 0$, Eq. (11) has two solutions in a specific range of the quantities b and ΔP_i: R_1 and R_2 (Fig. 1), where R_1 corresponds to a stable bubble, and R_2 to an unstable equilibrium of the bubble. Thus, all vapor–gas bubbles with radius $R < R_2$ have a stable shape $R = R_1$, and for $R > R_2$ there will be unlimited growth. When there is no gas in the bubble Eq. (11) has the simpler form

$$\Delta P_i = 2\sigma/R \tag{12}$$

and there is unique unstable solution: $R_V = 2\sigma/\Delta P_i$; then all the vapor bubbles with radius less than the critical value $R < R_V$ will collapse, while bubbles with radius $R > R_V$ will grow without limit.

The solution to Eq. (12) can be written in the form

$$R_v/R_{ef} = 2/\left(1 + \frac{(\partial P/\partial T)_s}{\sigma/R_{ef}}\Delta T_в\right). \tag{13}$$

In the absence of temperature overheat of the liquid $R_V = 2R_{ef}$, i.e., the critical curvature of the bubble is the curvature of the interphase artery-vapor channel surface. For low-temperature heat pipes, operating, as a rule, in the increased pressure region, the derivative $(dP/dT)_s$ is large, and therefore, even small overheats lead to a considerable variation in the critical radius.

The solutions of Eq. (11) are determined by the excess vapor pressure ΔP_i and the value of b, which, in turn, depend on the amount of gas m in the bubble. One must consider the influence of each of these factors. With increase in ΔP_i the curve P_i of excess pressure of the vapor–gas mixture rises upwards, and the solutions R_1 and R_2 become close, while R_1 increases and R_2 decreases. Thus, with increase of ΔP_i the growth in the amount of gas in the bubble corresponds to a rise in the curve of P_i and has the same consequences as in the previous case. Finally, one must consider the case of degeneracy of the two solutions into one: $R = R_*$, which corresponds to tangency of the hyperbola and can be determined from the system

$$\Delta P_i^* + \frac{b^*}{R_*^3} = \frac{2\sigma}{R_*}, \quad \frac{3b^*}{2\sigma R_*^2} = 1. \tag{14}$$

From the last equation of the system, which describes equality of the derivatives at the point of tangency of the hyperbola, it follows that

$$R_* = \left(\frac{9\bar{R}}{8\pi}\frac{m^*T^*}{\sigma}\right)^{1/2}, \tag{15}$$

i.e., R_*, being the upper limit of the parameter R_1, describing a stable state of the bubble, and the lower limit of the parameter R_2, describing an unstable state, is determined by the amount of gas, the temperature, and the surface tension coefficient. The parameter R_* depends on the type of heat-transfer agent, via the latter parameter.

By solving the system of equations (14), one can obtain an equation determining the relationship between the critical parameters:

$$\left(\frac{81\bar{R}}{128\pi}\frac{T^*m^*}{\sigma^3}\right)^{1/2}\Delta P_i^* = 1. \tag{16}$$

By introducing the function

$$F(m,\ \Delta P_i,\ T) = \left(\frac{81\bar{R}}{128\pi}\frac{Tm}{\sigma^3}\right)^{1/2}\Delta P_i, \tag{17}$$

one can determine the state of the bubble–liquid system from the value of this function.

$F > 1$. There is no solution to Eq. (11), an existing vapor–gas bubble is unstable, and there is unbounded growth; drying out of the arteries is unavoidable.

$F = 1$. There is a unique solution of the system, corresponding to an equilibrium state. Drying of the artery occurs if there is a deviation from the equilibrium state in the direction $R > R_*$.

$0 < F < 1$. There are two solutions of the equation: The first corresponds to a stable state of the system, and the second to an unstable state. A vapor–gas bubble is in the artery in a stable state $R = R_1$, and the artery dries out for an increase in the bubble size $R > R_2$.

$F \leq 0$, $m \neq 0$. There is a unique solution corresponding to a stable state of the system. A deviation of the bubble size from the design value does not cause drying out of the artery.

$F = 0$, $m = 0$, $\Delta P_i > 0$. The unique solution of Eq. (11) corresponds to an unstable state of the system. If the gas bubble deviates from equilibrium, the artery collapses or dries out.

$F = 0$, $m = 0$, $\Delta P_i \leq 0$. There is no solution of Eq. (11). A vapor bubble formed during filling of the artery collapses independently of its size.

From Eq. (16), knowing the relation $\sigma(T)$, we can determine the temperature dependence of the product $(m^*)^{1/2}\Delta P_i^*$. For example, for Freon 14 [11] we have

$$\sigma = B\left(1 - \frac{T}{T_{cr}}\right)^{1,27}. \tag{18}$$

A similar relation exists for Freon 22, and it differs only in the value of the coefficient B.

According to Eq. (16),

$$(m^*)^{1/2}\Delta P_i^* \sim \sigma^{3/2}(T^*)^{1/2} \tag{19}$$

or, allowing for Eq. (18),

$$(m^*)^{1/2}\Delta P_i^* \sim \left(1 - \frac{T^*}{T_{cr}}\right)^{1,9}\left(\frac{T_{cr}}{T^*}\right)^{1/2} = \varphi(T^*). \tag{20}$$

Thus, the temperature dependence of the product $(m^*)^{1/2} \times \Delta P_i^*$ for the heat-transfer agents F-14 and F-22 is described by the function φ (Fig. 2), and the latter decreases with increase in temperature. If there is no overheat of the liquid ($\Delta T_B = 0$), from Eqs. (6) and (16) we can obtain

$$R_{ef}^* = \left(\frac{81}{128}\frac{\bar{R}T^*m^*}{\pi\sigma}\right)^{1/2}. \tag{21}$$

From the last equation it is easy to determine conditions where bubbles with a known mass of gas cause drying of the capillary system.

Thus, the behavior of bubbles in heat pipe arteries can be represented as follows. Vapor–gas bubbles formed during filling of an artery lead to a slow drying out of the system, if their size exceeds a quantity R_2, which is determined for each heat-transfer agent by the temperature, the excess pressure of the vapor–gas mixture, and the mass of gas enclosed in the bubble. If $\Delta P_i \leq 0$, then $R_2 = \infty$. In the opposite case, where $R < R_2$, vapor–gas bubbles come to a stable equilibrium state under the influence of surface tension forces: Subsequent behavior of a bubble is determined by the dynamics of diffusion processes of solution of the gas and the operating conditions. With an increase in the excess vapor pressure $R = R_1$, due, e.g., to an increase in power or to a change in the slope of the pipe, bubbles with the least mass of gas grow, come close to the critical state ΔP_i, and when they reach this the force equilibrium is perturbed and drying of the arteries occurs. The relationship between the critical parameters is determined by the equality $F = 1$.

2. Methods of Increasing the Capabilities of Arterial Heat Pipes. From the foregoing, it follows that the influence of vapor–gas bubbles shows up, in the best case, in an increase to hydraulic resistance, and in the worst case, in drying out of the arterial system. Vapor bubbles can be condensed if there is a drop in temperature or a decrease in the excess vapor pressure R_*. A drop in temperature corresponds to a growth in the surface tension coefficient, and therefore, in the forces which tend to condense the vapor bubble. A decrease in the excess pressure can be effectively achieved by supercooling of the arterial liquid. In order to decrease the influence of vapor–gas bubbles, the authors of [6] used a supercooling effect and also perforated disks that inhibit the generation of bubbles in the most hazardous section, the evaporation zone.

In gas-filled heat pipes the process of bubble collapse is determined not by condensation of the vapor, but solution of the gas. The dynamics of solution are described by processes of saturation of the liquid with gas in the condenser and diffusion of gas from the liquid to the vapor channel. While the collapse of vapor bubbles can be accomplished in a short time, solution of vapor–gas bubbles is quite a slow process. Therefore, it is desirable to remove vapor–gas bubbles during filling of the arteries with liquid. An adaptation to allow a high-grade filling is suggested in [4], consisting of the use of a perforated foil from which the artery is filled in a certain section (usually in the evaporation zone). A bubble present in the artery is separated from the vapor channel by liquid, filling the perforation (Fig. 3). For a certain ratio between the aperture diameter and the foil thickness the liquid menisci are tangential; i.e., the aperture is open and the vapor–gas mixture is drawn into the vapor channel. For successful use of this adaptation, one requires that the foil thickness is less than the perforation diameter, i.e., it is measured in microns for a wick with a high capillary head. In the heat pipes mounted on the communication satellite CS-1, a foil of thickness 15 μm was used. However, a thin foil is the least robust element in the construction of heat pipes. In addition, the meniscus at the rim of the apertures can change its shape, which does not eliminate the possibility of blocking the perforations with liquid even for low thickness.

We have proposed the following method for removing bubbles: prepare the arteries with perforated screens and freeze the heat pipe after filling the arteries with condensate. The freezing of the pipe leads to vaporization of the liquid from the perforations above the vapor–gas bubbles. Thus, a path is opened for drawing the

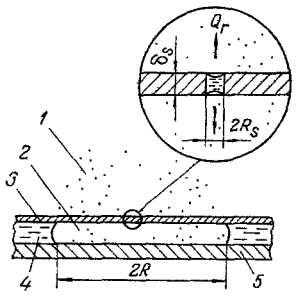

Fig. 3

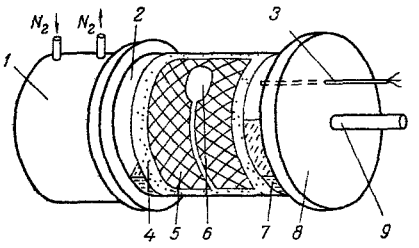

Fig. 4

Fig. 3. Closing of a vapor–gas mixture under a perforated screen: 1) vapor channel; 2) bubble; 3) screen; 4) liquid; 5) wall.

Fig. 4. Test section to determine the freezing required to remove a vapor–gas bubble: 1) chamber with liquid nitrogen; 2) glass cylinder; 3) thermocouple jacket; 4) perforated screen; 5) grid; 6) vapor–gas bubble; 7) working liquid; 8) lid; 9) vacuum line.

vapor–gas mixture into the vapor channel. By using this method for removing bubbles, the screen thickness can be quite large. We must explain the influence of various parameters on the freezing of the heat pipe.

Let a vapor–gas bubble of diameter 2R be in the gap between the heat pipe wall and a perforated screen of thickness δ_S with pore diameter $2R_S$.

When the pipe temperature is decreased, freezing of the screen above the bubble and the liquid in the perforations occurs due to vaporization of the latter. Assuming that for a large porosity the liquid temperatures in the perforations and the surrounding cells of the screen are the same, we can obtain the following equation for calculating the freezing:

$$\left[(1-\varepsilon)\frac{\rho_s c_{ps}}{\rho_l c_{pl}}+1\right]c_{pl}m_l dT = r dm_l, \tag{22}$$

which reflects the fact that freezing of the screen cells and the liquid located in the perforations occurs due to the heat of phase transformation during vaporization of the liquid. The last equation is integrated from the initial T_0 to the final temperature T of the pipe, and the mass of liquid in the perforations is reduced from m_{l0} to m_l. The solution in integral forms has the form

$$\Delta T = T_0 - T = \frac{r}{c_{pl}\left[1+(1-\varepsilon)\dfrac{\rho_s c_{ps}}{\rho_l c_{pl}}\right]}\ln\frac{m_{l0}}{m_l}. \tag{23}$$

The top limit of the freezing can be calculated from the assumption that in the initial state the liquid completely fills the volume of the pore, and the meniscus at the inferface is flat. The final volume is determined by the condition that the menisci link up, which corresponds to the moment of opening of the pore. The final mass depends on the angle of wetting θ of the screen by liquid. In calculating the final mass one must take into account variation in the volume of heat-transfer agent with the temperature. It can be seen from Eq. (23) that the freezing decreases with increase of the mass heat capacity of the cell $\rho_S c_{ps}$ and with decrease of the porosity ε. An increase in the screen thickness leads to an increase in the initial amount of liquid in the vapor; i.e., the ratio m_l/m_{l_0} falls, and ΔT increases. It follows from Eq. (23) that ΔT does not depend on the cooling time.

In the case where $(1-\varepsilon)\rho_S c_{ps}/\rho_l c_{pl} \to 0$, Eq. (23) takes the form

$$\Delta T = \frac{r}{c_{pl}}\ln\frac{m_{l0}}{m_l}, \tag{24}$$

from which it can be seen that it is impossible to accomplish complete vaporization of the liquid.

The effect of vaporization of liquid from the perforation and drawing out of the vapor–gas bubble from the capillary system was investigated experimentally by the authors. A general view of the test section is given in Fig. 4. The shell 2 of the working cylinder of diameter 40 mm was transparent, which allowed the

moment of withdrawal of the bubble to be determined visually. Freezing was controlled by passing liquid nitrogen through the chamber 1. The temperature in the working volume was measured with a copper–Constantan thermocouple, mounted in jacket 3. Between the wall and the perforated screen, made of stainless steel of thickness $\delta_s = 0.2$ mm, with surface porosity $\varepsilon = 0.5$ and aperture radius $R_s = 0.15$ mm, there was a layer of stainless woven mesh of thickness 0.2 mm. The mesh served to space the screen from the wall, and also to locate the vapor–gas bubble 6, by means of a slot provided for this. The gravitational overheat of the bubble was controlled by displacing the liquid 7 by rotating the equipment around its longitudinal axis. After the working section was charged with liquid (ethyl alcohol) it was cooled to $T \simeq 200°K$, and subsequently the gas introduced into the working volume through the lid 8 was partially pumped out through the nozzle. Then the section was brought to operating condition at $T = 343°K$. At the start of the experiment the screen and the mesh were wetted by immersing them in the liquid. Then hydrostatic drying was carried out for the gap in region 6, where the liquid rising along the slot closed off the vapor–gas during the subsequent filling. The bubble with $R \simeq 4$ mm formed and reached a state of stable equilibrium, determined by Eq. (11). After holding this section in a steady-state condition by supplying liquid nitrogen to chamber 1, the working volume was frozen until the pore opened and the vapor–gas mixture was drawn out from the wick.

According to a calculation, from Eq. (23) with initial value m_{l_0} corresponding to complete filling of the perforation, and final m_l corresponding to tangency of the menisci, the value of the freezing is $\Delta T = 70°K$. However, the experimentally obtained value of ΔT fell in the range 30-50°K. This overestimate of the theoretical data is evidently associated with an inexact choice of the original value of initial filling of the perforation m_{l_0}.

Thus, tests have shown that the use of perforated screens, together with prior chilling, allows one to remove vapor–gas bubbles from the arteries, which makes possible a considerable increase in the power level of heat pipes.

NOTATION

b	is the group in the gas equation of state;
B	is the coefficient;
c_l	is the linear heat capacity;
c_{ps}	is the heat capacity of the screen;
c_{pl}	is the heat capacity of the liquid;
F	is the state function of the vapor–gas bubble–liquid system;
m	is the number of moles of gas in the bubble;
m_{l_0}, m_l	are the initial and final quantity of liquid in a perforation;
P	is the pressure;
P_{vB}, P_{gas}	are the partial pressure of vapor and gas in a bubble;
P_i	is the excess pressure function for the vapor–gas mixture;
P_l	is the pressure of the liquid surrounding the bubble;
ΔP_g	is the gravitational pressure drop;
ΔP_l	is the drop in pressure due to circulation of liquid;
ΔP_T	is the pressure drop due to temperature overheat of the liquid;
ΔP_i	is the excess vapor pressure;
ΔP_σ	is the pressure drop due to the action of capillary forces;
$(\partial P/\partial T)_s$	is the pressure gradient on the saturation curve;
Q_r	is the heat flux removed from a perforation by evaporation;
R_{ef}	is the radius of curvature of the liquid meniscus at the interphase boundary of the artery-vapor channel;
R	is the bubble radius;
R_1 and R_2	are the radii of the vapor–gas bubble in a state of stable and unstable equilibrium, respectively;
R_v and R_*	are the critical radii of the vapor and vapor–gas bubbles;
R_s	is the radius of perforations in the screen;
$\bar{R}$	is the universal gas constant;
T	is the temperature;
T_0	is the initial temperature;
T_{cr}	is the temperature corresponding to the critical point on the liquid–vapor phase transformation line;

ΔT is the amount of cooling;
ΔT_B is the temperature overheat of the liquid;
ρ_l, ρ_s are the density of the liquid and the screen material;
r is the heat of vaporization;
σ is the surface-tension coefficient;
δ_s is the screen thickness;
φ is the temperature function;
θ is the wetting angle;
ε is the porosity.

The subscript * corresponds to solution of the system of equations (14).

LITERATURE CITED

1. P. R. Mock, B. D. Marcus, and E. A. Edelman, "Communication technology satellite: variable conductance heat pipe application," AIAA Paper N74-749 (1974).
2. W. Harwell, F. Edelstein, R. McIntosh, and S. Ollendorf, "Orbiting astronomical observatory heat pipe high performance data," AIAA Paper N73-758 (1973).
3. F. Edelstein, B. Swerdling, and R. Kosson, "Development of a self-priming high-capacity heat pipe for flight on OAO-C," Prog. Astro. Aeron., 31, 19 (1973).
4. Y. E. Eninger, "Meniscus coalescence as a mechanism for venting noncondensible gas from heat pipe arteries," AIAA Paper N74-748 (1974).
5. E. W. Saaski, "Gas occlusion in arterial heat pipes," AIAA Paper N724 (1973).
6. R. Kosson, R. Hembach, F. Edelstein, and J. Loose, "Development of a high-capacity variable-conductance heat pipe," AIAA Paper N73-728 (1973).
7. V. I. Subbotin, M. I. Ivanovskii, V. P. Sorokin, V. V. Privezentsev, and A. I. Strozhkov, "Degradation of heat pipe performance by vapor and vapor–gas bubbles," Teplofiz. Vys. Temp., 13, No. 6, 1225 (1975).
8. A. Abhat, M. Groll, and M. Hage, "Investigation of bubble formation in arteries of gas-controlled heat pipes," AIAA Paper N655 (1975).
9. G. I. Voronin (editor), Low-Temperature Heat Pipes for Aircraft [in Russian], Mashinostroenie, Moscow (1976).
10. E. I. Nesis, "New ideas in the physics of boiling," Fourth All-Union Conference on Heat and Mass Transfer, Minsk (1972).
11. V. F. Tomanovskaya and B. E. Kolotova, Freons: Properties and Uses [in Russian], Khimiya, Leningrad (1970).